ChemComm

Accepted Manuscript

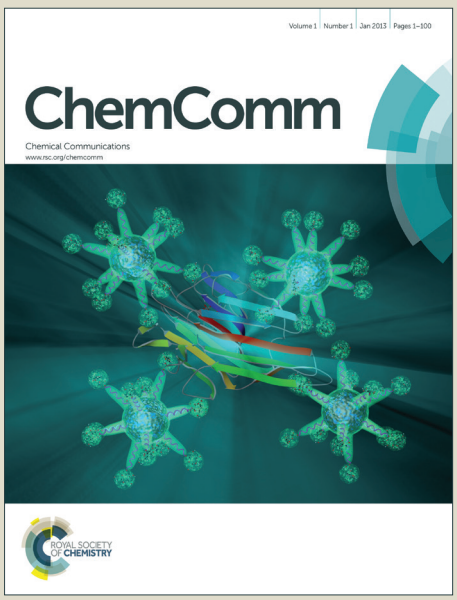

ROYAL SOCIETY OF CHEMISTRY

www.rsc.org/chemcomm

Journal Name

RSCPublishing

COMMUNICATION

A Dual-Boron-Cored Luminogen Capable for Sensing and Imaging

Cite this: DOI: 10.1039/x0xx00000x

Yubin Fu,[‡,a] Feng Qiu,[‡,a] Fan Zhang,*[a] Yiyong Mai,[a] Yingchao Wang,[b] Shibo Fu,[b] Ruizhi Tang,[a] Xiaodong Zhuang [a] and Xinliang Feng*[a,c]

Received 00th January 2012,
Accepted 00th January 2012

DOI: 10.1039/x0xx00000x

www.rsc.org/

A new dual-boron-cored luminogen ligated with nitrogen-containing multidentate ligand and four bulky phenyl rings, was readily synthesized. The unique molecular structure renders this BN-containing luminogen with rich photophysical properties in either solution or in solid state, including a large Stokes shift, aggregation induced emission activity and reversible piezochromism. Furthermore, this BN-containing luminogen exhibits good capabilities for imaging living cells and sensing of fluoride anion.

B,N-containing dyes, such as boron dipyrromethene (BODIPY), which exhibit high thermal stability, large charge carrier mobility and rich photophysical properties, have attracted increasing attention owing to their fundamental importance and potential applications in organic solar cells (OSCs), organic light-emitting diodes (OLEDs), sensing and imaging, etc.[1] However, these dye molecules mostly suffer from weakly emissive or nonemissive characters in concentrated solution or in solid state because of their small Stokes shifts, favourable for the self-absorption from the heavy overlap between the absorption and emission spectra, or the aggregation-caused fluorescence quenching (ACQ) effect.[2]

Aggregation-induced emission (AIE) has been considered as an effective strategy to achieve high emission in concentrated solution or even in solid state.[2b] Structurally dependent on the molecular conformation or solid-state packing, an AIE luminogen may response to a stimulation of mechanical performance, thus giving rise to the piezochromism behavior.[3] In contrast to the well-investigated AIE luminogens which are based on carbon-rich molecules, such as tetraphenylethene, AIE-active BN-containing luminogen remains rarely explored.

Boron-containing luminogens are widely used for sensing environment-harmful fluoride ions, featuring low detection limits, high selectivity and low-cost. Typically, the luminescence response works through the following driving forces: (1) hydrogen bonding interactions; (2) anion−π interactions; (3) F^- direct binding to boron atom; and (4) chemical reactions induced by F^-.[4] In this respect, searching for novel type of luminogens for fluoride anion sensing through a new responsive pathway, has been always an attractive topic.[5]

Herein, we report a novel dual-boron-cored luminogen **5**, through complexing 3,6-di(*1H*-pyrazol-1-yl)-1,2-diaminobenzene (**4**), a nitrogen-containing multidentate ligand with triphenylborane. The geometric structure and photophysical properties of **5** were fully characterized. We further investigated the capabilities of **5** for imaging living cells and selective sensing of fluoride anion.

The target compound **5** was synthesized as shown in Scheme 1. The reaction of 2,1,3-benzothiadiazole (**1**) with bromine gave 4,7-dibromo-2,1,3-benzothiadiazole (**2**) in 88% yield. The key intermediate 4,7-di(*1H*-pyrazol-1-yl)benzo-[2,1,3]thiadiazole (**3**) was prepared in a yield of 72% by copper iodide catalyzed reaction of **2** with pyrazole. Subsequently, compound **4** was obtained in quantitative yield upon reduction of **3** with $NaBH_4$. Finally, compound **4** and triphenylborane were treated in toluene under reflux condition, affording the target BN-complex **5** in 88% yield. Compound **5** was fully characterized by ^1H, ^{13}C, ^{11}B NMR and HRMS spectroscopies (Fig. S1-S7, ESI†). In the ^1H NMR spectra, only one set of proton signals in the aromatic regions and one N-H peak at 3.97 ppm can be observed (Fig. S5, ESI†), suggesting a symmetric structure of **5**. Moreover, the ^{11}B NMR spectrum manifests a signal peak at -7.9 ppm (Fig. S7, ESI†), indicative of a four-coordinated state of the boron center.[6]

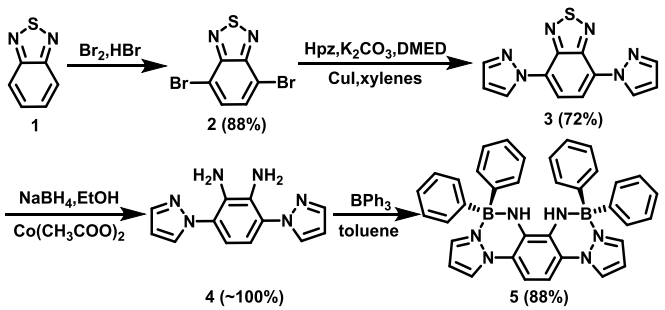

Scheme 1. Synthetic route towards compound **5**.

Single crystals of compound **5**, grown from acetone/n-hexane solution, were determined by single X-ray diffraction analysis (Fig. 1, Fig. S8-S9, ESI†). The crystal structure reveals a five-ring fused conjugated aromatic framework, in which two boron atoms are deviated from the mean plane of the backbone. The dihedral angles

defined by the middle benzene ring from two pyrazole rings, are 7.9° and 24.5°, respectively. Such twisted conformation can be attributed to the congested circumstance caused by the bulky diphenyl groups decorated on each boron core. Two kinds of B-N bonds with the lengths of 1.51/1.52 Å and 1.61/1.62 Å coincide with their covalent and coordination bond nature, respectively.[7] In the packing diagram, the molecules organize in a staggered stacking pattern. The conjugated backbones of the neighbouring molecules are parallel to each other in an edge-to-edge fashion, with the shortest distances from 3.35 to 3.95 nm between the neighbouring molecules. The intermolecular C-H•••π interactions (2.814 Å) between the phenyl groups and conjugated backbones of the adjacent molecules can be identified (Fig. 1b).

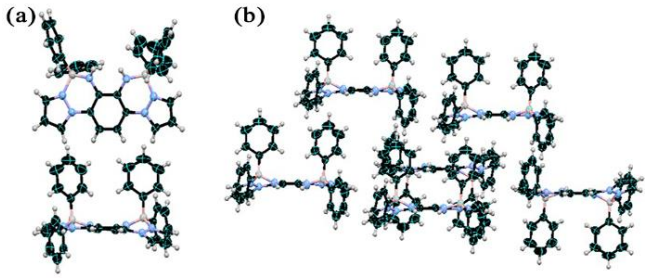

Fig. 1. (a) Thermal ellipsoid (50%) diagram of the molecular structure of **5**; (b) Crystal packing diagram of **5**. Solvent molecules are omitted for clarity.

The optical properties of compound **5** were investigated in CH_2Cl_2 at a concentration of 5×10^{-5} M (Fig. S10, ESI†). In the UV-vis spectra, three main absorption bands at 280, 329 and 394 nm were observed. The maximum absorption is typically attributed to the π–π* transition of the aromatic skeleton.[8] When compound **5** was dissolved in higher polar solvents, the peak at 394 nm is gradually red shifted to 415 nm (Fig. S10, ESI†), indicating an intramolecular charge transfer transition (CT). Thus, compound **5** can be polarized in the ground state. Such a phenomenon might be attributed to the multiple interactions between **5** and the solvent molecules, for instance, dipole-dipole, hydrogen bonding (through N-H moiety) and π-π interactions.[9] This result agrees with the time-dependent density functional theory (TD-DFT) calculation, which reveals that the CT peak at 394 nm governs the electron transition from the highest occupied molecular orbital (HOMO) to the lowest unoccupied molecular orbital (LUMO) (Fig. S14, ESI†). The fluorescence spectrum of compound **5** shows a broad emission with a maximum peak at 486 nm, featuring an unmirror image relative to the absorption spectrum. This suggests a lack of rigidity of the molecular scaffold.[10] Moreover, compound **5** in different solvents exhibits significant changes in emission maxima and intensity (Fig. S11, ESI†). The solvent-dependent emission of **5** is probably arising from its acceptor-donor-acceptor (A-D-A) character. The dipole moment of the molecule will be affected by different polar solvents, leading to the different stability of the excited state. It should be emphasized that, the Stokes shift of 92 nm (2081 cm^{-1}) for **5** is among the largest values ever reported for BN-containing luminophores.[7] This result indicates a remarkable structural deformation between the ground and excited states for compound **5**, which would be beneficial to achieve high emission efficiency through effective weakening of self-absorption.

Encouraged by the unique photophysical properties of compound **5**, next we like to explore its stimuli-response behavior. The emission spectra of **5** in THF/water with different volumetric ratios of water were recorded in Fig. 2. In a THF solution, the fluorescence spectrum of **5** shows a flat line parallel to the abscissa, manifesting the poor fluorescence behavior. Interestingly, the fluorescence intensity increases rapidly when the water content is above 50% (v/v), and it reaches to a maximum value at 80% (v/v) fraction of water, but then decreases at the higher fractions of water. This result strongly suggests a solvent-dependant AIE response.[2] To gain an insight into the aggregation behavior of compound **5**, the UV-vis spectra of **5** in THF/water solution with different volumetric ratios of water were recorded (Fig. S15, ESI†). The UV-vis spectra in aqueous THF with 80% and 90% of H_2O exhibit broadening absorption maxima with a levelling-off of long-wavelength tails, which are typically attributed to the formation of aggregates.[11,12] The aggregation behavior of **5** in THF/water was further supported by electron diffraction (ED) patterns and scanning electron microscope (SEM) images. The ED patterns disclose an amorphous state for the sample formed in THF-water mixed solutions with 70% or 80% of H_2O. In contrast, a crystalline state was obtained in the case of THF-water mixture with 90% of H_2O. This phenomenon is different from that of crystallization-induced emission enhancement (CIEE) effect.[13]

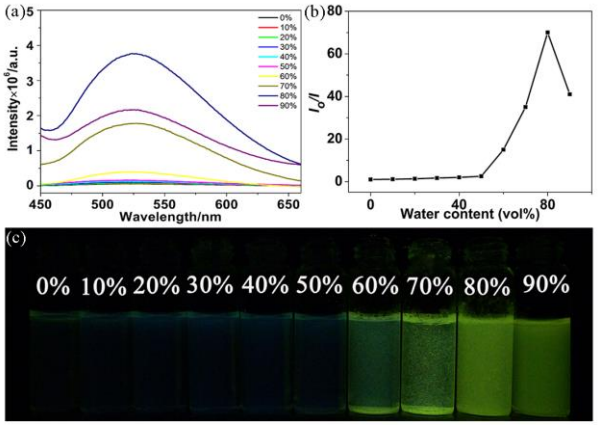

Fig. 2. (a) Fluorescence spectra of **5** in THF/water mixtures (1.0×10^{-3} M, excited at 413 nm) with varied volumetric fractions of water; (b) The fluorescence intensity change at different content of water; (c) The digital figures of **5** in THF/water mixtures under UV light (1.0×10^{-3} M, excited at 365 nm).

Compound **5** shows good photostability under the UV lamp (Fig. S18, ESI†). Moreover, the low in vitro cytotoxicity of **5** up to 100 μg mL^{-1} has been evaluated by MTT assay using NIH/3T3 normal cells (Fig. S19, ESI†). Thus, **5** with low cytotoxicity and AIE activity could be used as potential tool for biological imaging. The cellular uptake of compound **5** was evaluated by fluorescence microscope. As shown in Fig. 3, the strong blue fluorescence attributed to the aggregates of compound **5** was observed mainly in the cytoplasm of the cells with good distribution after culturing tumor cells with **5** for 2 h. With the increase of incubation time, the emission intensity in tumor cell increases (Fig. S20, ESI†), suggesting that the as-prepared nanoparticles were enclosed by the cell membranes, and then internalized by the cells. This result demonstrates that the structural feature of compound **5** with AIE activity is a good candidate for bioimaging applications.

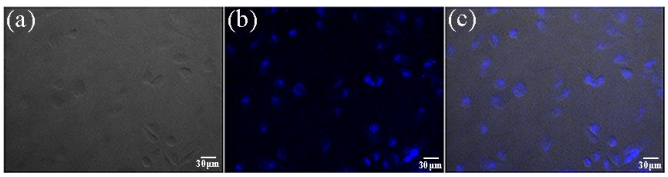

Fig. 3. Fluorescence microscope images of HeLa cells incubated with compound **5** for 2 h**:** (a) a bright field image; (b) a fluorescence image; (c) a merged image.

Piezochromic luminogens generally refer to color changes under external pressure or mechanical grinding[3e,3h] and have potential applications in optical recording devices, pressure sensors and damage detectors, etc.[3d,3f] We consider that the sterically congested structure of compound **5** which plays the key role in its AIE activity, may render the response to mechanical stimuli. To this end, we grinded the solid powder of **5** using a pestle. Interestingly, a change of emission color from green to yellow was observed under UV light at 365 nm (Fig. 4a, Fig. S21, ESI†). After one drop of dichloromethane was dropped onto the surface of the ground sample, the area that dichloromethane evaporated immediately recovered the original green color under UV light. Such reversible conversion of the emission colors of the as-prepared and ground samples can be successively repeated for several times (>4) as shown in Fig. 4b. The red-shifted emission color after mechanical grinding indicates the change of intermolecular interaction in solid **5**. To confirm the optical results, the crystal packing of 5 was further investigated by X-ray diffraction (XRD) measurements. XRD patterns disclose that the as-prepared and ground samples of **5** are featured with crystalline and amorphous phases, respectively, which demonstrates the change of molecular packing during the grinding process.[3f] This result also is reversible by alternately grinding and soaking with CH_2Cl_2 (Fig. 4c).

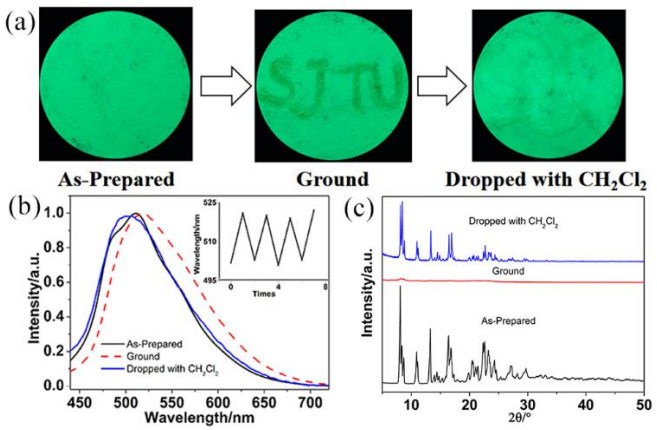

Fig. 4. (a) Photographic images of compound **5** after mechanical grinding under 365 nm UV light; (b) The solid fluorescence of compound **5**, Inset: repeated switching of the fluorescence emission maxima of the as-prepared and ground samples; (c) Powder XRD patterns of compound **5**.

The boron-cored structure of compound **5** also promoted us to examine its response to the stimuli of various anions. In the DMSO solution, compound **5** with a concentration of 5×10^{-5} M exhibits strong blue fluorescence which can be attributed to the high viscosity of solvent. Further addition of F^- (5×10^{-3} M) resulted in an apparent color change from colorless to light yellow (Fig. 5). Moreover, UV-vis absorption revealed that a profile comprising two absorption maxima at 294 and 334 nm with remarkably enhanced intensity emerged when F^- was added, while the fluorescence was fully quenched (Fig. S22-S24, ESI†). On the contrary, the addition of other anions (e.g. Cl^-, Br^-, I^-, NO_3^-, HSO_4^-) did not cause obvious changes of the absorption and fluorescence spectra. To determine the sensitivity of **5** to F^- ion, fluorescence titration experiment was carried out (Fig. S25, ESI†). With the incremental addition of F^-, the fluorescence intensity of **5** decreased progressively. The addition of 20 eq F^- resulted into a complete fluorescence quenching. This pronounced fluorescence response of **5** to F^- ion at such a low concentration (Fig. S26, ESI†), is comparable to the best F^- detectors reported previously, such as triarylboranes and aryltrifluoroborate.[14]

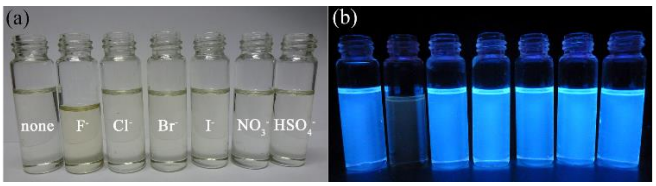

Fig. 5. Digital figures of compound **5** at a concentration of 5×10^{-5} M in DMSO under sunlight (a) and 365 nm UV light (b).

In order to understand the mechanism of fluoride anion sensing, we further carried out ^{1}H NMR titration experiments of **5** in DMSO-d_6. Upon addition of F^-, pronounced shifts of the proton signals were observed (Fig. 6). Upon gradually increasing the amount of F^- from 1 to 6 eq, the well-resolved proton signals in pyrazol ring (signed as H-a, H-b, H-d in Fig. 6a) and in BN moiety (H-e) became weaken and finally disappeared. Meanwhile, new proton signals at δ = 8.07, 7.77, 6.68 and 6.50 ppm emerged and their intensities increased. Strikingly, both chemical shifts and integration ratios of these new peaks are quite similar to those values of the protons in the ligand **4** (Fig. 6). Thereby, it is reasonable to deduce that the new species with similar chemical composition to the ligand **4** were formed upon the addition of F^-. On the other hand, the proton signal of the BN moiety (H-e) at δ = 6.07 ppm in **5** disappeared after F^- titration, while a new high-field signal with the same integration intensity at δ = 5.28 ppm, was observed, which is very close to that of the proton in the imino group in **4** (δ = 5.26 ppm). This result suggests that the BN moiety is not fused in the aromatic backbone after the treatment with F^-. Moreover, the ^{11}B NMR spectrum of **5** treated with F^- shows a signal at δ = -5.73 ppm, which is characteristic for four-coordinated boron atom (Fig. S27, ESI†).[6] On the basis of these analyses, we suggest a possible pathway of F^--stimuli response for **5** as shown in Fig. 6b. Two F^- ions simultaneously attack the two Lewis acid boron centers of compound **5**, leading to the cleavage of B-N coordination bond and the formation of B-F bond. In other words, the two coordinated N atoms of pyrazole units in the ligand are released, while each boron core bearing two phenyl rings and one F atom, is linked with the imino group through B-N covalent bond. As a consequence, the original rigid conjugated backbone of compound **5** was destroyed, and the pyrazole unit with a released free lone pair of electrons on the N atom probably acted as a crucial role in quenching the fluorescence through electron trapping effect.[15]

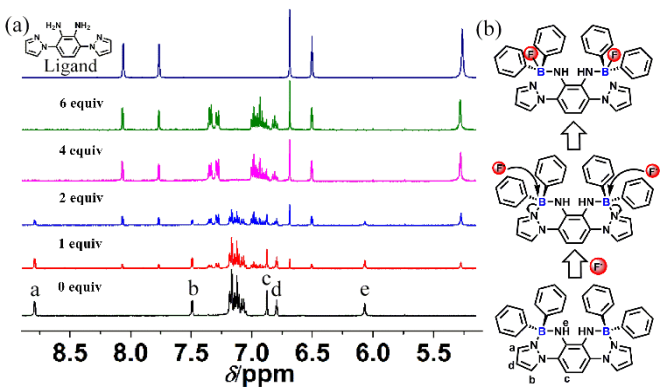

Fig. 6. (a) ^{1}H NMR spectra of boron compound **5** in DMSO-d_6 after the addition of various equivalents of TBAF; (b) Schematic representation of a possible mechanism of the reaction between compound **5** and F^- in DMSO.

Conclusions

In summary, we have synthesized a novel BN-containing luminogen, featuring a sterically congested conformation and an extended π-conjugated system. Remarkably, this luminogen exhibits a large

Stokes shift, AIE activity and reversible piezochromism behavior, etc. For a boron-based F^- detector, its boron center is required to be shielded with bulky substituents, e.g. dury group.[16] In this work, the boron core is effectively protected by binding a pyrazole moiety through a weak B-N coordination bond, which can be readily cleaved upon treatment with F^-. Such strategy holds great promise for designing new boron-based molecular dyes for sensing a wide scope of ions.

We thank the Natural Science Foundation of China (NSFC 21174083, 2012CB933400, 2013CBA01600), the Shanghai Committee of Science and Technology (11JC1405400), the FNRS, China Postdoctoral Science Foundation (2013M540356). We thank Dr. Manfred Wagner from Max Planck Institute for Polymer Research for NMR analysis, and Dr. Wangzhang Yuan from Shanghai Jiao Tong University for kind discussion about AIE effect and mechanochromism.

Notes and references

[a]School of Chemistry and Chemical Engineering, Shanghai Jiao Tong University, Shanghai 200240, P. R. China.
E-mail: fan-zhang@sjtu.edu.cn
[b]The first hospital Jilin University, College of Basic Sciences of Jilin University, Changchun 130021, P. R. China
[c]Department of Chemistry and Food Chemistry & Center for Advancing Electronics Dresden (cfaed), Technische, Universitaet Dresden, Mommsenstrasse 4, 01062 Dresden, Germany;
E-mail: xinliang.feng@tu-dresden.de

†X ray crystallographic data for compound **5** (CCDC 1031193), can be obtained free of charge from The Cambridge Crystallographic Data Centre via http://www.ccdc.cam.ac.uk/data request/cif ; Electronic Supplementary Information (ESI) available: Experimental details, optical spectra, DFT calculation, NMR spectra, cellular imaging . See DOI: 10.1039/c000000x/

‡These two authors contributed equally to this work.

1. (a) M. J. G. Lesley, A.Woodward, N. J. Taylor, T. B. Marder, I. Cazenobe, I. Ledoux, J. Zyss, A. Thornton, D. W. Bruce and A. K. Kakkar, *Chem. Mater.*, 1998, **10**, 1355; (b) C. D. Entwistle and T. B. Marder, *Chem.Mater.*, 2004, **16**, 4574; (c) C. D. Entwistle and T. B. Marder, *Angew. Chem., Int. Ed.*, 2002, **41**, 2927; (d) S. Wang, *Coordin. Chem. Rev.*, 2001, **215**, 79.
2. (a) X. Cheng, D. Li, Z. Zhang, H. Zhang and Y. Wang, *Org. Lett.*, 2014, **16**, 880; (b) Y. Hong, J. W. Y. Lam and B. Z. Tang, *Chem. Soc. Rev.*, 2011, **40**, 5361; (c) Y. Hong, J. W. Y. Lam and B. Z. Tang, *Chem. Commun.*, 2009, 4332.
3. (a) W. Liu, Y. Wang, M. Sun, D. Zhang, M. Zheng and W. Yang, *Chem. Commun.*, 2013, **49**, 6042; (b) D. Zhao, G. Li, D. Wu, X. Qin, P. Neuhaus, Y. Cheng, S. Yang, Z. Lu, X. Pu, C. Long and J. You, *Angew. Chem. Int. Ed.*, 2013, **52**, 13676; (c) Y. Sagara, T. Mutai, I. Yoshikawa and K. Araki, *J. Am. Chem. Soc.*, 2007, **129**, 1520; (d) Y. Sagara and T. Kato, *Nat. Chem.*, 2009, **1**, 605; (e) H. Bouas-Laurent, H. Dürr, *Pure Appl. Chem.*, 2001, **73**, 639; (f) K. Nagura, S. Saito, H. Yusa, H. Yamawaki, H. Fujihisa, H. Sato, Y. Shimoikeda and S. Yamaguchi, *J. Am. Chem. Soc.*, 2013, **135**, 10322; (g) X. Zhang, Z. Chi, J. Zhang, H. Li, B. Xu, X. Li, S. Liu, Y. Zhang and J. Xu, *J. Phys. Chem. B*, 2011, **115**, 7606; (h) Y. Dong, B. Xu, J. Zhang, X. Tan, L. Wang, J. Chen, H. Lv, S. Wen, B. Li, L. Ye, B. Zou and W. Tian, *Angew. Chem. Int. Ed.*, 2012, **51**, 10782; (i) X. Gu, J. Yao, G. Zhang, Y. Yan, C. Zhang, Q. Peng, Q. Liao, Y. Wu, Z. Xu, Y. Zhao, H. Fu and D. Zhang, *Adv. Funct. Mater.*, 2012, **22**, 4862; (j) N. Zhao, Z. Yang, J. W. Y. Lam, H. H. Y. Sung, N. Xie, S. Chen, H. Su, M. Gao, I. D. Williams, K. S. Wong, B. Z. Tang, *Chem. Commun.*, 2012, **48**, 8637; (k) Y. Dong, J. W. Y. Lam, A. Qin, Z. Li, J. Sun, H. H. Y. Sung, I. D. Williams, B. Z. Tang, *Chem. Commun.*, 2007, 40; (l) X. Luo, J. Li, C. Li, L. Heng, Y. Q. Dong, Z. Liu, Z. Bo, B. Z. Tang, *Adv. Mater.*, 2011, **23**, 3261.
4. (a) Y. Zhou, J. F. Zhang and J. Yoon, *Chem. Rev.*, 2014, **114**, 5511; (b) C. Saravanan, S. Easwaramoorthi, C. -Y. Hsiow, K. Wang, M. Hayashi and L. Wang, *Org. Lett.*, 2013, **16**, 354; (c) W. -M. Wan, F. Cheng and F. Jäkle, *Angew. Chem., Int. Ed.*, 2014, **53**, 8934.
5. (a) C. R. Wade, A. E. J. Broomsgrove, S. Aldridge and F. P. Gabbaï, *Chem. Rev.*, 2010, **110**, 3958; (b) A. Roy, D. Kand, T. Saha and P. Talukdar, *Chem. Commun.*, 2014, **50**, 5510.
6. (a) Y. -s. Guo, F. Zhang, J. Yang, F. -f. Wang, Y. NuLi and S. -i. Hirano, *Energy Environ. Sci.*, 2012, **5**, 9100; (b) S. Bieller, F. Zhang, M. Bolte, J. W. Bats, H. -W. Lerner and M. Wagner, *Organometallics*, 2004, **23**, 2107.
7. J. F. Araneda, W. E. Piers, B. Heyne, M. Parvez and R. McDonald, *Angew. Chem., Int. Ed.*, 2011, **50**, 12214.
8. (a) Y. Liu, F. Zhang, C. He, D. Wu, X. Zhuang, M. Xue, Y. Liu and X. Feng, *Chem. Commun.*, 2012, **48**, 4166; (b) Z. -H. Guo, T. Lei, Z. -X. Jin, J. -Y. Wang and J. Pei, *Org. Lett.*, 2013, **15**, 3530.
9. R. Li, S. Xiao, Y. Li, Q. Lin, R. Zhang, J. Zhao, C. Yang, K. Zou, D. Li and T. Yi, *Chem. Sci.*, 2014, **5**, 3922.
10. X. Wang, F. Zhang, J. Liu, R. Tang, Y. Fu, D. Wu, Q. Xu, X. Zhuang, G. He and X. Feng, *Org. Lett.*, 2013, **15**, 5714-5717.
11. (a) Y. Zhang, D. Li, Y. Li and J. Yu, *Chem. Sci.*, 2014, **5**, 2710; (b) X. Zhu, R. Liu, Y. Li, H. Huang, Q. Wang, D. Wang, X. Zhu, S. Liu and H. Zhu, *Chem. Commun.*, 2014, **50**, 12951.
12. C. He, D. Wu, F. Zhang, M. Xue, X. Zhuang, F. Qiu and X. Feng, *ChemPhysChem*, 2013, **14**, 2954.
13. (a) Y. Yang, X. Su, C. N. Carroll and I. Aprahamian, *Chem. Sci.*, 2012, **3**, 610; (b) Z. Zhao, S. Chen, X. Shen, F. Mahtab, Y. Yu, P. Lu, J. W. Y. Lam, H. S. Kwok and B. Z. Tang, *Chem. Commun.*, 2010, **46**, 686; (c) Y. Dong, *In Aggregation-Induced Emission: Fundamentals and Applications, Volumes 1 and 2*, John Wiley and Sons Ltd2013, pp 323; (d) L. Qian, B. Tong, J. Shen, J. Shi, J. Zhi, Y. Dong, F. Yang, Y. Dong, J. W. Y. Lam, Y. Liu and B. Z. Tang, *J. Phy. Chem. B*, 2009, **113**, 9098; (e) Y. Dong, J. W. Y. Lam, A. Qin, J. Sun, J. Liu, Z. Li, J. Sun, H. H. Y. Sung, I. D. Williams, H. S. Kwok and B. Z. Tang, *Chem. Commun.*, 2007, 3255; (f) Y. Jin, Y. Xu, Y. Liu, L. Wang, H. Jiang, X. Li and D. Cao, *Dyes Pigments*, 2011, **90**, 311.
14. (a) J. O. Huh, H. Kim, K. M. Lee, Y. S. Lee, Y. Do and M. H. Lee, *Chem. Commun.*, 2010, **46**, 1138; (b) R. Ting, C. Harwig, U. auf dem Keller, S. McCormick, P. Austin, C. M. Overall, M. J. Adam, T. J. Ruth and D. M. Perrin, *J. Am. Chem. Soc.*, 2008, **130**, 12045; (d) M. Nicolas, B. Fabre and J. Simonet, *Electrochim. Acta*, 2001, **46**, 3421.
15. R. Tang, F. Zhang, Y. Fu, Q. Xu, X. Wang, X. Zhuang, D. Wu, A. Giannakopoulos, D. Beljonne and X. Feng, *Org. Lett.*, 2014, **16**, 4726.
16. W. Zhao, X. Zhuang, D. Wu, F. Zhang, D. Gehrig, F. Laquai and X. Feng, *J. Mater. Chem. A*, 2013, **1**, 13878.

